VNU Journal of Science: Mathematics – Physics, Vol. 31, No. 4 (2015) 23-31

Synthesis and Optical Characterization of Samarium Doped Cerium Fluoride Nanoparticles

Duong Thi Mai Huong*, Nguyen Thi Tien, Le Van Vu, Nguyen Ngoc Long

Faculty of Physics, VNU University of Science, 334 Nguyen Trai, Thanh Xuan, Hanoi, Vietnam

Received 31 August 2015
Revised 22 October 2015; Accepted 20 November 2015

Abstract: CeF_3 nanoparticles doped with 0; 1.0; 1.5; 2.0; 2.5; 3.0 and 4.0 mol% Sm^{3+} were prepared by co-precipitation technique. These nanoparticles were studied by X-ray diffraction (XRD), transmission electron microscopy (TEM), photoluminescence (PL), photoluminescence excitation (PLE) spectra, energy-dispersive X-ray (EDS) and absorption spectra. The PL spectra exhibit a group of four emission lines, which are assigned to the transitions from the excited state $^4G_{5/2}$ to the ground states ^6H_J with J = 5/2; 7/2; 9/2 and 11/2 of Sm^{3+} ion. The intensity of PL related to Sm^{3+} ion reached to a maximum when the Sm dopant content was 2 mol%. The PLE spectra show 8 lines, which are attributed to the absorption transitions from the $^6H_{5/2}$ ground state to the $^4H(1)_{9/2}$, $^4D(2)_{3/2}$, $^6P_{7/2}$, $^4F(3)_{7/2}$, $^6P_{5/2}$, $^4M_{17/2}$, $^4I(3)_{13/2}$ and $^4M_{15/2}$ excited states. Six lines among eight excitation lines were observed in the diffuse reflection spectra.

Keywords: Co-precipitation, samarium doped cerium fluoride, nanopaticles, absorption, photoluminescence.

1. Introduction

Lanthanide fluorides have been applied in luminescence devices, such as sensor, displays, fluorescent lamps, scintillators, up-converters, optical amplifiers and lasers. Lanthanide fluorides provide some special advantages, such as high resistivity, excellent thermal and environmental stability, and in particular, these materials possess very low vibrational energies, e.g., phonon energy in lanthanum fluoride (LaF_3) is about 350 cm^{-1}, which will decrease the non-radiative rate and thus increase the luminescence intensity [1]. Among these lanthanide fluorides, cerium fluoride (CeF_3) nanostructures have promising applications as inorganic scintillators, luminescent host materials as well as solid lubricants [2]. In addition, CeF_3 nanoparticles shows Faraday effect, which is applicable to optoelectronics such as an optical isolator, optical switches or optical memory [3].

* Corresponding author. Tel.: 84-988648823
Email: maihuongk12@gmail.com

With the development of nanotechnology, many techniques have been developed to synthesize CeF_3 nanostructures such as thermal decomposition [1], hydrothermal [2,4], polyol [3,5], reverse micelles [6], precipitation [7,8], sonication assisted [9], sol-gel [10] and microemulsion [11]. CeF_3 nanostructures with varying morphology, such as nanoparticles [1,3,5-10], core/shell nanoparticles [1,4,5,8], nanocages, nanorings [2], nanoplates [4], nanodiskettes [11], etc, have been fabricated using a variety of growth methods.

It is well-known that the rare-earth (RE) ions have sharp absorption and emission bands from the UV to infrared range. For that reason, the RE doped materials possess potential applications in many different fields such as optoelectronics, photonics and biomedicine applications. However, to the best of our knowledge, for CeF_3 most of previous studies have been focused only on doping CeF_3 with terbium ion (Tb^{3+}) [1,4,5,11]. Samarium (Sm^{3+}) ion is an important luminescent center, which is doped in many glasses [see, for example, 12]. However, the optical properties of Sm^{3+}- doped CeF_3 (CeF3:Sm^{3+}) nanoparticles have not been reported before.

In this report, we fabricated CeF_3:Sm^{3+} nanoparticles by co-precipitation method. The structure, absorption, PL and PLE properties of the samples are investigated in detail.

2. Experimental

Undoped and Sm^{3+}- doped CeF_3 nanoparticles were prepared by co-precipitation method from cerium nitrate $Ce(NO_3)_3$, samarium nitrate $Sm(NO_3)_3$ solution and NH_4F powder. An appropriate amount of NH_4F was dissolved in ethanol under constant stirring for 15 min to prepare NH_4F solution. In a typical synthesis, stoichiometric amounts of $Ce(NO_3)_3$ and $Sm(NO_3)_3$ aqueous solutions were mixed. The molar ratio of Sm:Ce was equal to 0; 1.0; 1.5; 2.0; 2.5; 3.0 and 4.0 mol% Sm^{3+}. Then, appropriate amounts of NH_4F solution were added into the mixed nitrate solution under stirring for 3 h at room temperature. After that, the resulting precipitate was filtered off and washed many times in water and ethanol to remove chemicals remaining in the final products. The last products were dried in air at 70 ^oC for 4 h.

Crystal structure of the obtained powders was analysed by X-ray diffraction (XRD) using an X-ray diffractometer SIEMENS D5005, Bruker with Cu $K\alpha_1$ (λ = 1.54056 Å) irradiation. The surface morphology of the samples was observed by using a JEOL JEM 1010 transmission electron microscope (TEM). The composition of the samples was determined by an energy-dispersive X- ray spectrometer (EDS) OXFORD ISIS 300. The room temperature PL and the PLE spectra were carried out on a spectrofluorometer Fluorolog FL 3-22 Jobin-Yvon-Spex with a 450 W xenon lamp as an excitation source. Diffuse reflection measurements were carried out on a UV-VIS-NIR Cary-5000 spectrophotometer. The spectra were recorded at room temperature in the wavelength region of 300-600 nm. Absorption spectra of the samples were obtained from the diffuse reflectance data by using the Kubelka-Munk function [13]:

$$F(R) = \frac{(1-R)^2}{2R} = \frac{K}{S}$$

where *R*, *K* and *S* are the reflection, the absorption and the scattering coefficients, respectively.

3. Results and Discussions

3.1. Structure characterization and morphology

Typical XRD patterns of CeF_3 nanoparticles doped with 0; 1.0; 1.5; 2.0; 2.5; 3.0 and 4.0 mol% Sm^{3+} are presented in Fig.1. In all case, the powder XRD analysis evidenced that the obtained CeF_3 samples have a hexagonal crystal structure. No diffraction peaks of the other material phase are detected. The lattice constants of the CeF_3 nanocrystals determined from the XRD patterns are a = 7.12 ± 0.02 Å and c = 7.28 ± 0.01 Å, which are in good agreement with the standard values a = 7.112 Å and c = 7.292 Å (JCPDS 08-0085). The average size of the nanocrystals was estimated by Debye-Scherrer's formula [14]:

$$D = \frac{0.9\lambda}{\beta \cos\theta}$$

where β is the full width at half maximum (FWHM) in radians of the diffraction peaks, θ is the Bragg's diffraction angle and λ = 0.154056 nm. The calculated size of the CeF_3 nanocrystals was estimated to be 14 nm.

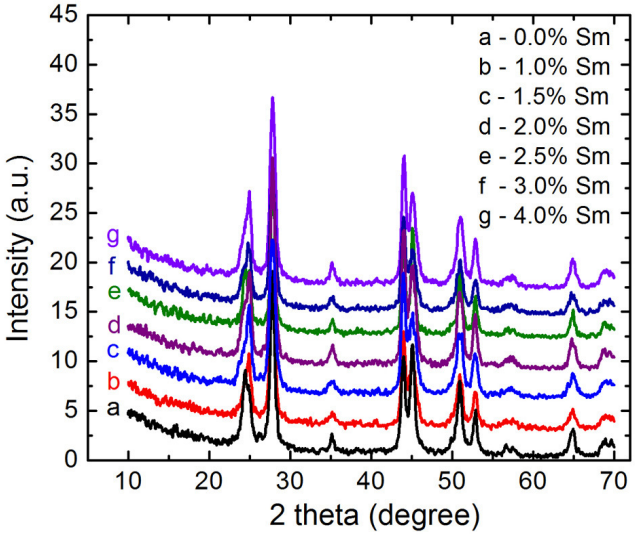

Figure 1. XRD patterns of the CeF_3 nanoparticles doped with different Sm^{3+} contents.

TEM image of the 2 mol% Sm^{3+}- doped CeF_3 samples are illustrated in Figure 2.

As can be seen from the image, the samples CeF_3 are composed of nanoparticles. The size of the CeF_3:2 mol% Sm^{3+} nanoparticles ranges from 15 to 25 nm, which are slightly bigger than that calculated by Debye-Scherrer's formula.

The result of EDS analysis for the CeF_3 nanopowders doped with different Sm^{3+} contents is given in Table 1. The undoped CeF_3 nanoparticles mainly consist of cerium (Ce), fluor (F) elements,

whereas in the CeF_3:1%Sm^{3+} and CeF_3:3%Sm^{3+} samples Sm element appeared, indicating the incorporation of Sm^{3+} ions into the host lattice. It is noted that the oxygen (O) observed in the EDS spectra is the residual not totally removed during washing.

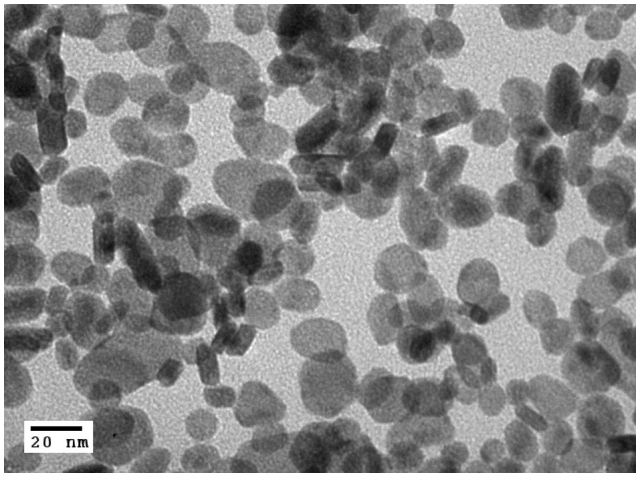

Figure 2. TEM image of the CeF_3 nanoparticles doped with 2 mol% Sm^{3+}.

Table 1. Chemical composition of CeF_3 nanoparticles doped with different Sm^{3+} contents.

Element	Sample		
	CeF_3:0%Sm	CeF_3:1%Sm	CeF_3:3%Sm
O (at.%)	8.55	11.58	10.66
F (at.%)	66.09	62.36	63.07
Ce (at.%)	25.36	24.48	23.98
Sm (at.%)	0	1.58	2.29

It is known that effective radii of Ce^{3+} and Sm^{3+} ions in hexagonal crystal are 1.48 and 1.38 Å, respectively [15]. It is expected that the Sm^{3+} ions can substitute for the Ce^{3+} ions in CeF_3:Sm^{3+} lattice because ionic radii for Ce^{3+} and Sm^{3+} are close. The second reason for this is that both Ce and Sm are RE metals, they possess similar chemical properties. Can be seen from table 1, the Ce atomic percentage decreases with increasing the Sm atomic percentage, which proves that the Sm^{3+} ions have substituted for the Ce^{3+} ions in CeF_3:Sm^{3+} lattice.

3.2. Photoluminescence and absorption properties

Figure 3 illustrates the room temperature PLE spectrum monitored at 594 nm emission line and the PL spectrum under excitation wavelength of 400 nm of the CeF_3 nanoparticles doped with 2 mol% Sm^{3+}. As will be seen below, the lines in the spectra are interpreted as the absorptive and radiative intra-configurational f-f transitions within the Sm^{3+} ions.

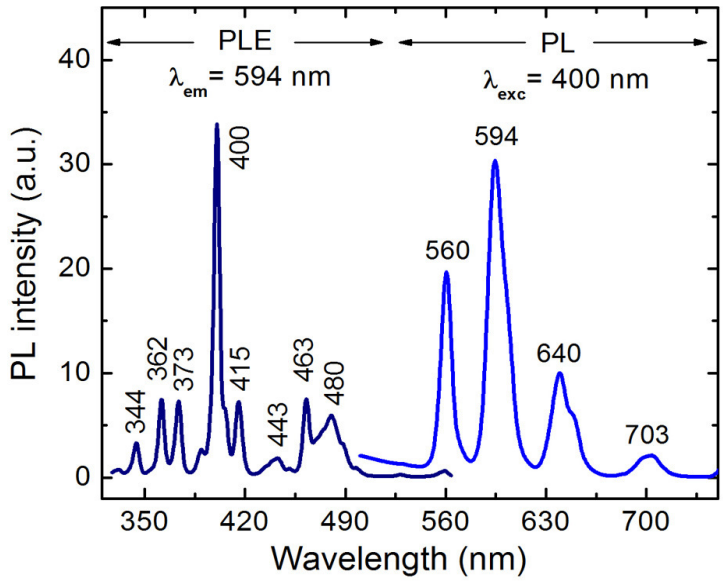

Figure 3. PL and PLE spectra of CeF_3:2mol%Sm^{3+}

The room temperature PL spectra of CeF_3 nanoparticles undoped and doped with 1.0; 2.0; 3.0 and 4.0 mol% Sm^{3+} excited by 400 nm wavelength are shown in figure 4.

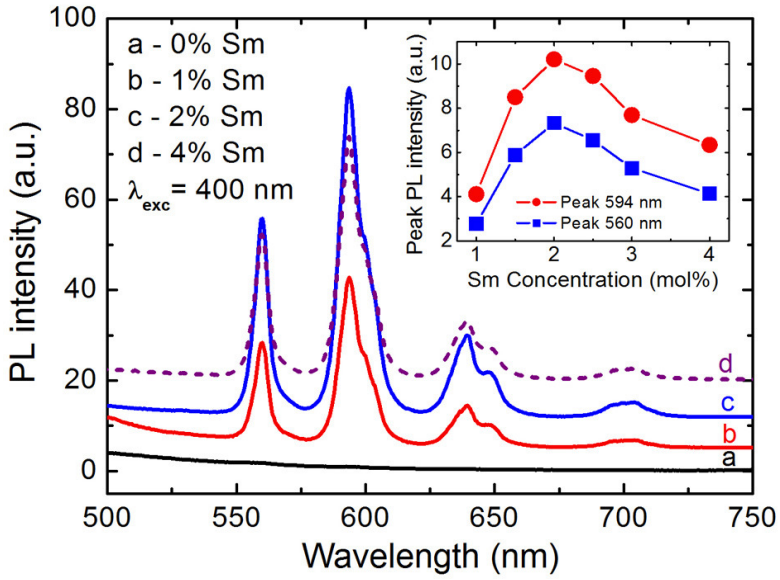

Figure 4. PL spectra of CeF_3 nanoparticles doped with different Sm^{3+} contents. The inset shows the intensity of 594 nm and 560 nm peaks as a function of Sm^{3+} concentration.

The undoped CeF_3 nanoparticles do not exhibit the groups of emission lines in the wavelength range from 525 to 750 nm, whereas the Sm^{3+}- doped CeF_3 nanoparticles show a group of four emission lines at 560, 594, 640 and 703 nm. The inset of figure 4 indicates that the intensity of PL related to Sm^{3+} ion reaches to a maximum when the Sm dopant content is 2 mol%.

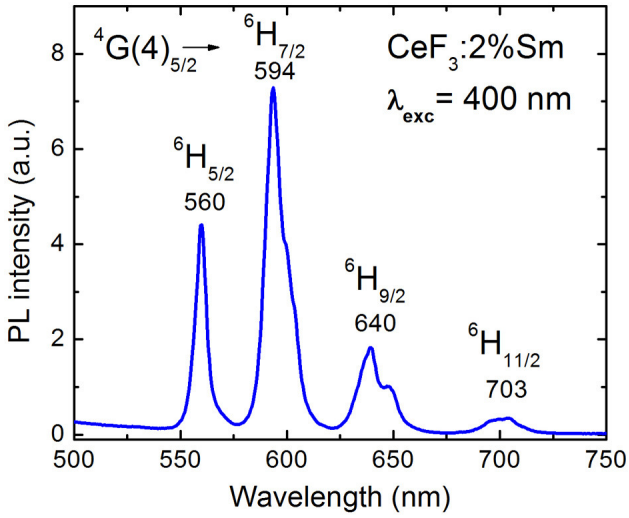

Figure 5. PL spectrum excited by 400 nm wavelength of CeF_3 nanoparticles doped with 2 mol% Sm^{3+}.

Figure 5 shows typical PL spectrum excited by 400 nm wavelength of 2 mol% Sm^{3+}- doped CeF_3 nanoparticles. The group of emission lines at 560, 594, 640 and 703 nm are assigned to the transitions from the excited state $^4G(4)_{5/2}$ to the ground states ^6H_J with J = 5/2; 7/2; 9/2 and 11/2 of Sm^{3+} ion, respectively.

It is worth noting that all the mentioned above emission lines have the same excitation spectra, which demonstrates that all these lines possess the same origin. Typical PLE spectrum monitored at 594 nm emission line of 2 mol% Sm^{3+}- doped CeF_3 nanoparticles is illustrated in figure 6. The excitation lines located at 344, 362, 373, 400, 415, 443, 463 and 480 nm are attributed to the absorption transitions from the $^6H_{5/2}$ ground state to the $^4H(1)_{9/2}$, $^4D(2)_{3/2}$, $^6P_{7/2}$, $^4F(3)_{7/2}$, $^6P_{5/2}$, $^4M_{17/2}$, $^4I(3)_{13/2}$ and $^4M_{15/2}$ excited states, respectively.

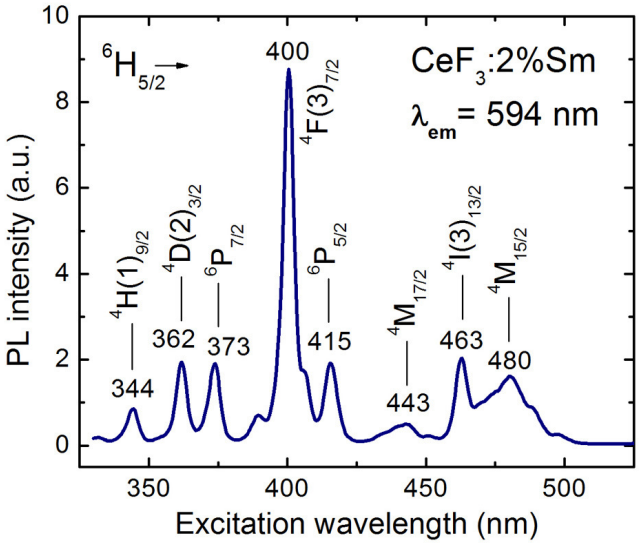

Figure 6. PLE spectrum monitored at 594 nm emission line of CeF_3 nanoparticles doped with 2 mol% Sm^{3+}.

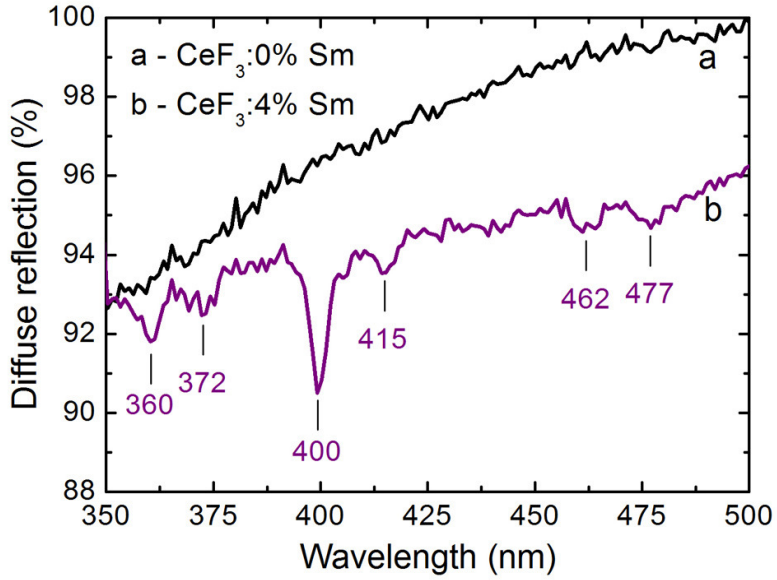

Figure 7. Diffuse reflection spectra at room temperature of the undoped and 4 mol% Sm^{3+}- doped CeF_3 nanoparticles.

Figure 7 depicts diffuse reflection spectra measured at room temperature of the undoped CeF_3 and the 4.0 mol% Sm^{3+}- doped CeF_3 nanoparticles. Can be seen that none of the absorption lines appears in the diffuse reflection spectrum of the undoped CeF_3 nanoparticles, while six weak absorption lines located at 360, 372, 400, 415, 462 and 477 nm are clearly observed in the spectrum of 4.0 mol% Sm^{3+}- doped CeF_3 nanoparticles.

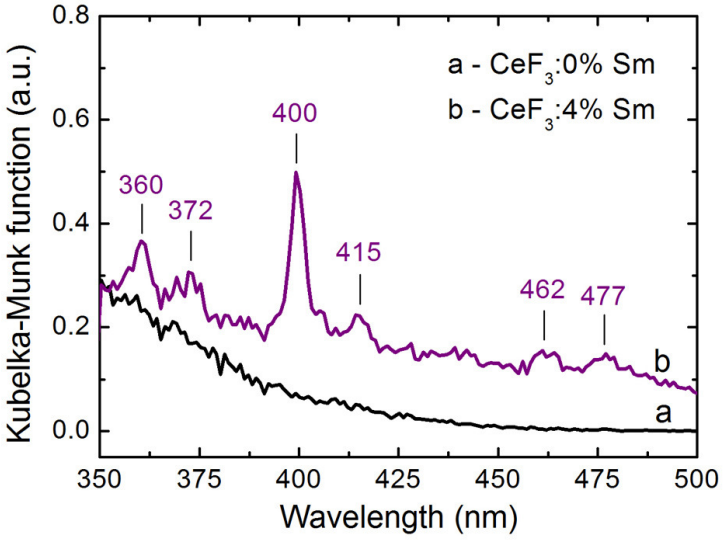

Figure 8. Plot of Kubelka-Munk function F(R) proportional to absorption coefficient for the undoped CeF_3 and the 4.0 mol% Sm^{3+}- doped CeF_3 nanoparticles.

Absorption spectra obtained from the diffuse reflectance data by using the Kubelka–Munk function F(R) for the undoped CeF_3 and the 4.0 mol% Sm^{3+}- doped CeF_3 nanoparticles are shown in figure 8. It is interesting to note that six mentioned above absorption lines observed in the plot of Kubelka-Munk function have appeared in the excitation spectra as shown in figure 6. The absorption lines located at 360, 372, 400, 415, 462 and 477 nm are assigned to the optical transitions from the $^6H_{5/2}$ ground state to the $^4D(2)_{3/2}$, $^6P_{7/2}$, $^4F(3)_{7/2}$, $^6P_{5/2}$, $^4I(3)_{13/2}$ and $^4M_{15/2}$ excited states, respectively.

Conclusion

The Sm^{3+}- doped CeF_3 nanoparticles were prepared by co-precipitation method. The XRD analysis showed that the nanoparticles exhibit a pure hexagonal structure. TEM images show that CeF_3 nanoparticles have the size from 15 to 25 nm. The PL intensity is strongest in the CeF_3 samples doped with 2 mol% Sm^{3+}. The PL and PLE spectra of Sm^{3+} ions result from the optical intra-configurational f–f transitions. Some excitation lines were observed as well in diffuse reflection spectra measured at room temperature.

References

[1] Shili Gai, Piaoping Yang, Xingbo Li, Chunxia Li, Dong Wang, Yunlu Dai, Jun Lin, Monodisperse CeF3, CeF3:Tb3+, and CeF3:Tb3+@LaF3 core/shell nanocrystals: synthesis and luminescent properties, J. Mater. Chem. 21 (2011) 14610-14615.

[2] Qiang Wu, Ying Chen, Pei Xiao, Fan Zhang, Xizhang Wang, Zheng Hu, Hydrothermal Synthesis of Cerium Fluoride Hollow Nanostructures in a Controlled Growth Microenvironment J. Phys. Chem. C 112 (2008) 9604–9609.

[3] S. Eiden-Assmann, G. Maret, CeF_3 nanoparticles: synthesis and characterization, Mater. Res. Bull. 39 (2004) 21–24.

[4] Chunxia Li, Xiaoming Liu, Piaoping Yang, Cuimiao Zhang, Hongzhou Lian, Jun Lin, LaF_3, CeF_3, CeF_3:Tb^{3+}, and CeF_3:Tb^{3+}@LaF_3 (Core-Shell) Nanoplates: Hydrothermal Synthesis and Luminescence Properties, J. Phys. Chem. C 2008, 112, 2904-2910.

[5] Z.L. Wang, Z.W. Quan, P.Y. Jia, C. K. Lin, Y. Luo, Y. Chen, J. Fang, W. Zhou, C.J. O'Connor, J. Lin., A Facile Synthesis and Photoluminescent Properties of Redispersible CeF_3, CeF_3:Tb^{3+}, and CeF_3:Tb^{3+}/LaF_3 (Core/Shell) Nanoparticles, Chem. Mater. 2006, 18, 2030-2037.

[6] H. Lian, M. Zhang, J. Liu, Z. Ye, J. Yan, C. Shi, Synthesis and spectral properties of lutetium-doped CeF_3 nanoparticles, Chem. Phys. Lett. 395 (2004) 362–365.

[7] Máté Kovács, Zsolt Valicsek, Judit Tóth, László Hajba, Éva Makó, Pál Halmos, Rita Földényi, Multi-analytical approach of the influence of sulphate ion on the formation of cerium(III) fluoride nanoparticles in precipitation reaction, Colloids Surf., A 352 (2009) 56–62.

[8] Tomasz Grzyb, Marcin Runowski, Krystyna Dabrowska, Michael Giersig, Stefan Lis, Structural, spectroscopic and cytotoxicity studies of TbF_3@CeF_3 and TbF_3@CeF_3@SiO_2 nanocrystals, J. Nanopart. Res. 15 (2013) 1958 (15 pp).

[9] D. Arun Kumar, S. Selvasekarapandian, H. Nithya, Yoshitake Masuda, Structural and conductivity analysis on cerium fluoride nanoparticles prepared by sonication assisted method, Solid State Sci. 14 (2012) 626-634.

[10] J. del Castillo, A.C. Yanes, J. Mendez-Ramos, J.J. Velazquez, V.D. Rodrıguez, Structural and luminescent study in lanthanide doped sol–gel glass–ceramics comprising CeF_3 nanocrystals, J. Sol-Gel Sci. Technol. 60 (2011) 170–176.

[11] H. Guo, Photoluminescent properties of CeF_3:Tb^{3+} nanodiskettes prepared by hydrothermal microemulsion, Appl. Phys. B 84 (2006) 365-369.

[12] Sunil Thomas, Rani George, Sk. Nayab Rasool, M. Rathaiah, V. Venkatramu, Cyriac Joseph, N.V. Unnikrishnan, Optical properties of Sm^{3+} ions in zinc potassium fluorophosphates glasses, Opt. Mater. 36 (2013) 242–250.

[13] Phosphor Handbook edited under the Auspices of Phospor Research Society, editorial committee co-chairs: Shigeo Shionoya, William M. Yen, CRC Press, Boca Raton Boston London, Newyork, Washington DC, 1999, p. 763.

[14] B.E. Warren, X-ray Diffraction Dover publications Inc, New York, 1990, p. 253.

[15] R.D. Shannon, Revised effective ionic radii and systematic studies of interatomic distances in halides and chalcogenides, Acta Cryst. A32 (1976) 751-767.